Measuring the width of growth rings in tropical species using digital image processing: the case of *retrophyllum rospigliosii*

***Medición de ancho de anillos de crecimiento de especies tropicales usando procesamiento digital de imágenes, caso de* retrophyllum rospigliosii**

Medição da largura dos anéis de crescimento de espécies tropicais utilizando processamento digital de imagens: o caso de retrophyllum rospigliosii

Ricardo José Trullo Guerrero[1]
Carlos Alberto Gaviria López[2]
Jorge Andrés Ramírez Correa[3]

Received: October 10th, 2024
Accepted: December 15th, 2024
Available: May 5th, 2025

How to cite this article:
R.J. Trullo Guerrero, C.A. Gaviria López, and J.A. Ramírez Correa, "Measuring the Width of Growth Rings in Tropical Species Using Digital Image Processing: The Case of *Retrophyllum rospigliosii,*" *Revista Ingeniería Solidaria,* vol. 21, no. 2, 2025. doi: https://doi.org/10.16925/2357-6014.2025.02.04

Research article. https://doi.org/10.16925/2357-6014.2025.02.04

[1] Master's Student in Automation, Department of Robotics, Instrumentation and Control, Faculty of Electronic Engineering and Telecommunications, University of Cauca.
Email: rtrullo@unicauca.edu.co
ORCID: https://orcid.org/0009-0006-7127-8407
CvLAC: https://scienti.minciencias.gov.co/cvlac/visualizador/generarCurriculoCv.do?cod_rh=0000176556

[2] Professor, Department of Robotics, Instrumentation and Control, Faculty of Electronic Engineering and Telecommunications, University of Cauca.
Email: cgaviria@unicauca.edu.co
ORCID: https://orcid.org/0000-0002-9773-7660
CvLAC: https://scienti.minciencias.gov.co/cvlac/visualizador/generarCurriculoCv.do?cod_rh=0000348830

[3] Professor, Faculty of Agricultural Sciences, University of Cauca.
Email: j.ramirez@unicauca.edu.co
ORCID: https://orcid.org/0000-0003-3101-052X
CvLAC: https://scienti.minciencias.gov.co/cvlac/visualizador/generarCurriculoCv.do?cod_rh=0000684686

CC BY

Abstract

Introduction: This article presents the results of the research study "Evaluation of the Correlation Between the Anatomical Characteristics of Colombian Pine Wood (Retrophyllum rospigliosii) Extracted Through Computer Vision and the Climatic Information in the Center of the Cauca Department," conducted as part of a Master's program in Automation at the University of Cauca in 2023.

Objective: To assess the application of artificial vision techniques in measuring the width of growth rings of *Retrophyllum rospigliosii*.

Methods: Twenty cross-sections of Retrophyllum rospigliosii were obtained from plantations located in southwestern Colombia. The sections displayed annual growth rings, and the widths of these rings were measured.

Results: In the analyzed cross-sections, 20 annual rings—each corresponding to a year of plantation—were identified. The fully automatic method using a color difference gradient approach yielded a percentage error of 218.05%, detecting only four rings. In contrast, the semi-automatic method successfully identified all 20 growth rings, with an average percentage error of 29.42%.

Conclusions: The proposed semi-automatic method for measuring ring width using computer vision demonstrated significantly better performance than the fully automatic approach. The promising results highlight the potential of computer vision tools to identify growth rings and contribute to understanding the climatic history of tropical forests.

Originality: A semi-automatic method is proposed for marking and measuring growth rings in the Retrophyllum rospigliosii species.

Limitations: The accuracy of ring marking depends on the user's skill and expertise.

Key words: artificial vision; tropical conifer; automatic identification; pattern recognition; color gradient

Resumen

Introducción: El artículo es resultado del estudio de investigación "Evaluación de la correlación entre las características anatómicas de la madera de pino colombiano (*Retrophyllum rospigliosii*) extraídas mediante visión computarizada y la información climática en el centro del departamento del Cauca", realizado como parte de un programa de Maestría en Automatización en la Universidad del Cauca en 2023.

Objetivo: Evaluar la aplicación de técnicas de visión artificial en la medición del ancho de los anillos de crecimiento de Retrophyllum rospigliosii.

Métodos: Se obtuvieron veinte secciones transversales de *Retrophyllum rospigliosii* de plantaciones ubicadas en el suroeste de Colombia.

Resultados: En las secciones transversales examinadas, se discernieron 20 anillos anuales correspondientes a cada año de plantación. El enfoque de gradiente de diferencia de color resultó en un error porcentual del 218.05% en comparación con la medición manual con solo 4 anillos identificados, mientras que el enfoque semi-automático identificó los 20 anillos de crecimiento, obteniendo un error porcentual promedio del 29.42%.

Conclusiones: La medición semi-automática del ancho del anillo propuesta por visión computarizada muestra un rendimiento superior a nuestro intento de identificación completamente automática. Los buenos resultados obtenidos apuntan a la viabilidad de nuevas herramientas basadas en visión computarizada para identificar anillos de crecimiento y avanzar en la revelación de la historia climática de los bosques tropicales.

Originalidad: Se propone un método semi-automático para el marcado y medición de anillos de crecimiento en la especie *Retrophyllum rospigliosii*.

Limitaciones: El marcado de anillos de crecimiento depende de la habilidad y experiencia del usuario.

Palabras clave: visión artificial; conífera tropical; identificación automática; reconocimiento de patrones; gradiente de color

Resumo

Introdução: Este artigo é resultado do estudo de pesquisa "Avaliação da correlação entre as características anatômicas da madeira de pinheiro colombiano (Retrophyllum rospigliosii) extraída por meio de visão computacional e informações climáticas na região central do Departamento de Cauca", realizado como parte do programa de Mestrado em Automação da Universidade de Cauca em 2023.

Objetivo: Avaliar a aplicação de técnicas de visão computacional na medição da largura dos anéis de crescimento de *Retrophyllum rospigliosii*.

Métodos: Vinte seções transversais de *Retrophyllum rospigliosii* foram obtidas de plantações localizadas no sudoeste da Colômbia.

Resultados: Nas seções transversais examinadas, foram identificados 20 anéis de crescimento, correspondentes a cada ano de plantio. A abordagem por gradiente de cor apresentou um erro percentual de 218,05% em comparação com a medição manual, identificando apenas 4 anéis. A abordagem semiautomática, por outro lado, identificou todos os 20 anéis de crescimento, atingindo um erro percentual médio de 29,42%.

Conclusões: A medição semiautomática da largura dos anéis de crescimento, proposta por visão computacional, apresenta desempenho superior em comparação com nossa tentativa de identificação totalmente automática. Os resultados positivos obtidos apontam para a viabilidade de novas ferramentas baseadas em visão computacional para a identificação de anéis de crescimento e para o avanço da nossa compreensão da história climática das florestas tropicais.

Originalidade: Propõe-se um método semiautomático para marcação e medição de anéis de crescimento na espécie ⁎*Retrophyllum rospigliosii*⁎.

Limitações: A marcação dos anéis de crescimento depende da habilidade e experiência do usuário.

Palavras-chave: visão computacional; conífera tropical; identificação automática; reconhecimento de padrões; gradiente de cores.

1. INTRODUCTION

Reconstructing the climatic history of a place or region is essential for identifying recurring climatic patterns and long-term trends. Such analysis facilitates the study of phenomena like El Niño and La Niña, as well as the detection of climate change events [1]. Dendrochronology is a scientific technique that involves dating growth rings in woody plants to investigate and quantify environmental processes across various scientific disciplines, including climatology, ecology, geomorphology, and archaeology [2]. This is accomplished by analyzing features such as ring width, intra-ring wood density, isotope composition, pore density, and the total number of rings [3].

Dendrochronological studies in both temperate and tropical regions have demonstrated a strong correlation between tree ring width and environmental variables

such as precipitation, solar radiation, wildfires, and ambient temperature [4], [5]. These associations provide valuable insights into historical climatic conditions and allow for the assessment of human impacts on forest ecosystems. In this context, dendrochronological analyses serve as a critical tool for developing conservation strategies and mitigating adverse environmental effects [6], [7].

An illustrative example is the analysis of the Amazon River basin, where extended droughts and periods of high humidity were identified during the latter half of the 19th century. These climatic events have been partially attributed to anthropogenic activities, notably intensive deforestation. The validity of these findings was confirmed through rigorous statistical analysis, revealing a significant correlation ($r = 0.91$) between meteorological records from 1786 to 2016 and climatic variations inferred from tree ring data [8].

In recent years, the field of dendrochronology has seen promising developments through the integration of emerging technologies such as computer vision and artificial intelligence in the analysis of tree growth rings [9], [10]. These innovations offer significant potential to enhance the precision and efficiency of dendrochronological research. For instance, artificial vision combined with satellite imagery has been used to calculate a disturbance index in Picea engelmannii trees affected by beetle infestations. Dendrochronological data served as ground truth for evaluating the accuracy of the index in distinguishing healthy trees from those affected. Results showed an overall classification accuracy between 80% and 82%, and an accuracy of 59% to 71% in identifying beetle-killed trees [11].

Research on growth rings has traditionally focused on forests in mid- and high-latitude regions, where tree species tend to form well-defined rings that effectively record environmental and climatic variations [12]. In contrast, tropical trees are subject to irregular wet and dry seasons, as well as flooding, which can influence ring formation and often result in less distinct growth patterns [13], [14], [15].

In temperate zones, dendrochronological studies increasingly utilize automated techniques involving image acquisition tools such as scanners and cameras. These images are analyzed using algorithms like Sobel masks, gradient magnitude and angle detection, and artificial intelligence models to identify concentric growth rings [2], [16]. Commercial software tools, such as WinDendro [9], are available to identify and measure ring widths from digital images. In [10], Fabijańska et al. reported improvements in ring detection accuracy using thresholding techniques, which increased the detection rate from 43% to 87% compared to the CooRecorder program. However, these tools may struggle with accuracy when growth rings are faint or closely spaced [16], [17].

This study presents a novel approach for identifying and measuring growth rings using computer vision, addressing the specific challenges of detecting rings in tropical tree species [18], [19]. To this end, previously characterized samples of Colombian pine (Retrophyllum rospigliosii) from 20-year-old forest plantations were used. We evaluated the performance of two computer vision-based methods: a fully automatic method based on the gradient calculation of total color difference, and a semi-automatic method requiring user confirmation of candidate pixels as ring boundaries. The findings of this research aim to support future dendrochronological investigations in tropical regions and enhance historical climate records for predicting climatic phenomena and analyzing their impacts.

2. MATERIALS AND METHODS

Study Area: Samples were collected from an experimental plantation established for the restoration of Retrophyllum rospigliosii in the municipality of El Tambo, Cauca (2.48º N, 76.83º W). The plantation was established in 1999 at a density of 800 trees per hectare. No silvicultural interventions were conducted during the rotation period.

Cross section Extraction:

Cross-sections were extracted from 20 trees in 2020, taken at a height of 30 cm to ensure inclusion of all rings formed throughout the tree's lifetime. To enhance the visibility of growth rings, the sections were sanded using a sequence of abrasive papers with increasing grits (60, 100, 180, 360, 360, 400, 600, 1000, and 1200 grits per square inch) [20].

To measure the annual increment of Retrophyllum rospigliosii, radii were drawn from the pith to the bark on each cross-section to identify individual growth rings. The conventional method for marking and measuring ring widths was applied. Ring boundaries were manually verified using a ZEISS stereoscope with a 4× lens. The cross-sections were then digitized using an HP Deskjet F4280 scanner at a resolution of 1200 dpi. Ring widths were measured with ImageJ software, employing the ObjectJ plugin [21].

A method for automatically detecting and measuring the width of growth rings was employed:

The approach used the gradient of the total color difference to detect ring contours. This involved tracing n rays from the center of the trunk pith (as marked by the user) to the bark in the image. The rays were spaced at 10° intervals, resulting in a total of n =

36 rays to be analyzed. A radial increment Ir, determined by the image resolution, was also defined to divide each ray into m equally spaced points along the radial distance from the origin.

The cross-sectional image of the tree was transformed into the CIELab color space, which provides a perceptually uniform distribution of colors and closely resembles human color perception. This space represents color using three components: L, a, and b. The L component indicates lightness, while a and b correspond to color-opponent dimensions. This study employs the total color difference ΔE, as defined in Equation (1), which is based on the differences among the L, a, and b components. This method enables color variations perceived as similar to be translated into equivalent Euclidean distances within the CIELab space [22].

$$\Delta E = \sqrt{\Delta L^2 + \Delta a^2 + \Delta b^2} \quad (1)$$

The algorithm calculates the color difference ΔE(i) for each pair of pixels at radial distances Ir·i and Ir·(i+1) for i = 0...m−1 in each Lab channel, using the operator Δ to indicate the difference. The resulting ΔE series highlights high values where significant color differences occur, potentially indicating tree-ring boundaries. To identify these contours, we compute the positions of the peaks in the ΔE gradient using the 'gradient' and 'findpeaks' functions in MATLAB®.

To enhance peak detection accuracy and reduce noise, a third-order polynomial estimation is applied using the 'lpc' command. To assess the similarity between detected peaks, the maximum correlation between peak positions across adjacent rays in the color difference gradient is computed. This step serves to validate the position of candidate pixels as true ring contour edges.

Pixels exhibiting high color differences but lacking consistent patterns in neighboring rays are filtered out. Figure 1 illustrates this scenario by displaying the color difference series for three adjacent rays, each separated by 1°. It is evident that the peaks may not align across the three rays.

During the identification process, the radially computed candidate positions do not always correspond to Cartesian coordinates in the original image. To resolve this, the 'knnsearch' function in MATLAB® is used to locate the nearest pixel in the original image to the calculated radial position of each candidate pixel.

e-ISSN 2357-6014 / Vol. 21, no. 2 / may-august 2025 / Bogotá D.C., Colombia
Universidad Cooperativa de Colombia

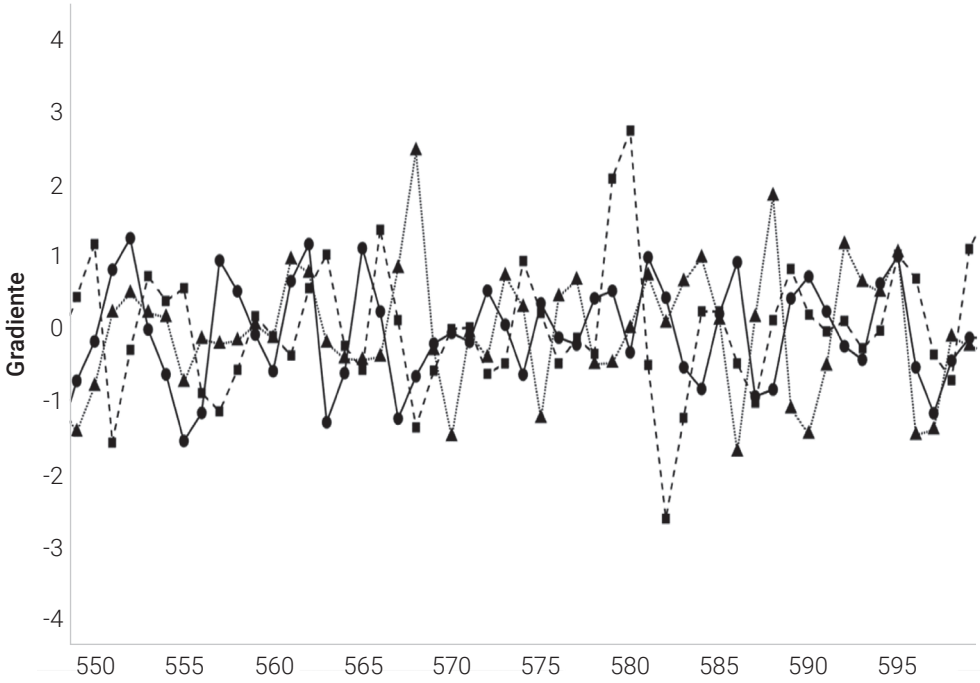

Fig 1. Gradient of color differences for rays corresponding to angles 10° (solid line), 11° (dashed line), and 12° (dotted line). Candidate positions are those with the highest correlation between adjacent rays.
Source: Authors.

The identification process of candidate contour pixels is repeated for all rays separated by 10°. Subsequently, a mathematical spline model is fitted for each contour using the fit command with the 'smoothingspline' option in MATLAB®, based on candidate pixels located at equal radial distances across the rays. This generates a predictive function for each contour that estimates the radial distance of a contour pixel as a function of its angular position.

Semi-automatic marking:

The image of the tree cross-section is divided into n radii, each defined from the central pixel of the trunk to its outer edge. The value of n is determined by the number of angular divisions (in polar coordinates) used to partition the 360° of the image. For each ring contour, candidate pixels are marked at every defined angle, from the innermost ring to the outermost. At each angle, the algorithm searches a region of interest (ROI) comprising the 9 neighboring pixels of the current location. This ROI is explored radially, starting either from the position of the previous contour or, in the case of the innermost contour, from the center of the trunk.

e-ISSN 2357-6014 / Vol. 21, no. 2 / may-august 2025 / Bogotá D.C., Colombia
Universidad Cooperativa de Colombia

Within each ROI, the algorithm presents the user with candidate pixels that meet specific criteria for contour inclusion. These candidate pixels are highlighted in red on the image. The user then interactively selects the correct contour pixel using the computer keyboard. The radial distance and angle of each selected pixel are recorded for further processing. Using these points, curve fitting in polar coordinates is performed to model the ring contours. The optimal contour fit is achieved using MATLAB®'s cubic spline interpolation. This process is repeated for each user-identified ring contour, beginning at the position of the previous ring and resulting in a mathematical model for each contour.

The edge detection process begins with identifying edge pixels in the original color image of the tree cross-section. To preserve edge integrity, we selected the local Laplacian filter, which is particularly effective for local enhancement without over-sharpening. This filter is applied to regions where ring edges are expected, helping reduce noise while preserving significant boundaries. MATLAB®'s 'locallapfilt' function provides access to this algorithm.

The image is first converted to the CIELab color space, and the L (lightness) channel is extracted. This channel is then normalized for mean and variance and smoothed using a Gaussian filter. Subsequently, the 'FrangiFilter2D' function is applied, which identifies pixels with the highest intensity gradients in all directions based on the eigenvalues of the Hessian matrix. This function is based on the work of Frangi et al. [23] and implemented in MATLAB® by [24].

To determine ring width, the Euclidean distance between successive ring contours along a given radius is measured. This distance, expressed in millimeters, represents the width of the growth ring.

3. RESULTS

The study analyzed a cross-section of the Retrophyllum rospigliosii species, manually identifying 20 growth rings and recording an average radial growth of 6.59 mm per year [25]. The evaluation metrics for the artificial vision techniques applied to tree core analysis include the number of rings identified and the accuracy of their corresponding width measurements.

Image Acquisition: Figure 2 displays the digital image of the cross-section of a Retrophyllum rospigliosii tree.

e-ISSN 2357-6014 / Vol. 21, no. 2 / may-august 2025 / Bogotá D.C., Colombia
Universidad Cooperativa de Colombia

Fig. 2. Cross-sectional cut of a tree from the species Retrophyllum rospigliosii. The image was acquired using a optic scanner at a resolution of 2400 dpi.
Source: Authors.

Figure 3 presents the grayscale image of a Retrophyllum rospigliosii tree cross-section, highlighting the pixel intensity information associated with growth rings. The grayscale intensities of pixels within and outside the growth rings are notably similar, generally ranging from 139 to 149. Specifically, pixels within the growth rings exhibit intensities of 149, 148, and 139, while pixels outside the rings show intensities of 149 and 147. This minimal contrast poses a challenge for ring detection based solely on grayscale intensity.

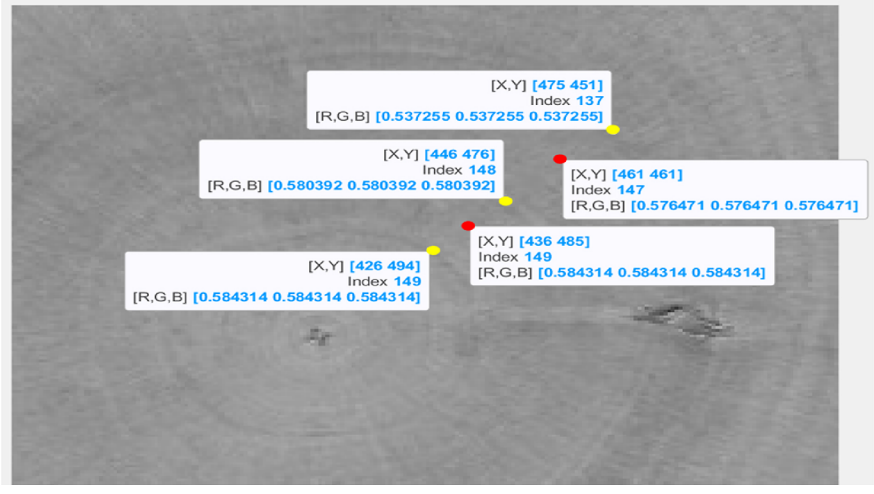

Fig. 3. Digital image of a cross-sectional cut of a Retrophyllum rospigliosii tree. Yellow points indicate pixels identified as part of the growth rings, while red points represent pixels outside the growth rings. For each point, the image shows the Cartesian coordinates and the corresponding grayscale intensity value (Index).
Source: Authors.

Manual marking: The growth rings were manually identified and marked, resulting in a total of 20 rings. The rings shown in Figure 4 were used to quantify the annual increment of Retrophyllum rospigliosii. Radii extending from the pith to the bark were delineated in both transverse and radial directions to identify and measure the width of each growth ring. The rings were carefully traced along the entire tree circumference in the transverse sections to consolidate the collected data [25].

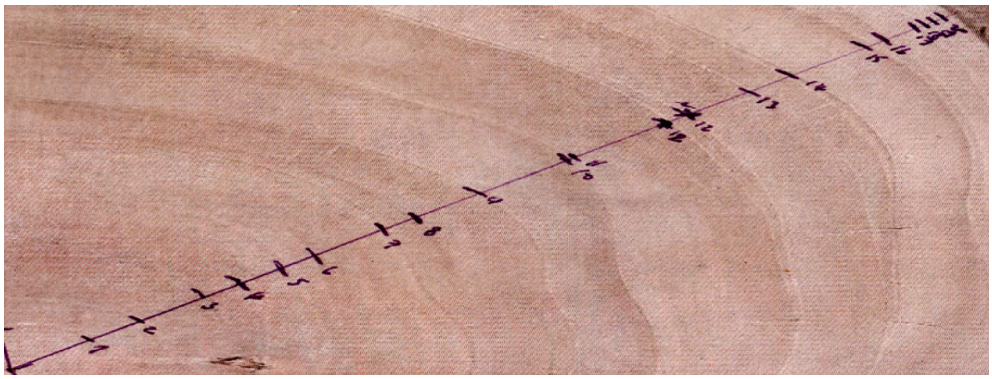

Fig. 4. Manual marking of growth rings in the species Retrophyllum rospigliosii.
Source: Authors.

The growth rings of Retrophyllum rospigliosii were identified by examining the complete cross-section of the tree. At the macroscopic level, discontinuous or spurious rings were observed. The availability of the full cross-section allowed for the projection of multiple rays, which facilitated the identification of diffuse growth rings. These irregularities are attributed to the lobed growth pattern of the tree, a phenomenon influenced by prevailing climatic conditions [25].

Automatic marking: Figure 5 displays the outcome of processing the digital image of the cross section of the Retrophyllum rospigliosii tree using the 'Sobel' algorithm in MATLAB. Incomplete contours in some growth rings are identified, as well as 'scars' in the wood, such as the one visible near the center of the cross section.

e-ISSN 2357-6014 / Vol. 21, no. 2 / may-august 2025 / Bogotá D.C., Colombia
Universidad Cooperativa de Colombia

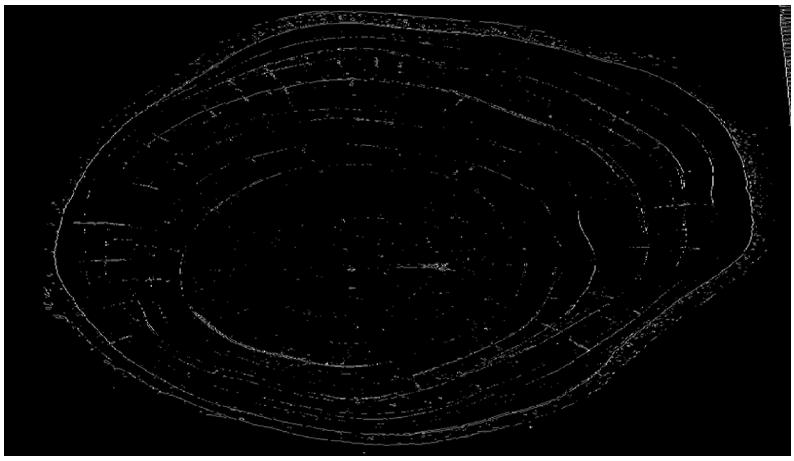

Fig. 5. Image of the cross-sectional cut of the tree from the species Retrophyllum rospigliosii processed using the 'Sobel' edge detection algorithm in MATLAB.
Source: Authors.

The total color difference gradient method was also applied. Figure 6 presents a magnified region of the cross-section, illustrating the results of this method. Black pixels indicate the locations of detected color difference gradient peaks. Red pixels—sometimes overlapping with black or blue ones—represent points with a high correlation between adjacent radii. Blue pixels correspond to the k-nearest neighbors identified during the spatial refinement process. The combined use of correlation analysis and the nearest-neighbor approach enables the elimination of gradient peak points that do not correspond to consistent patterns in adjacent rays.

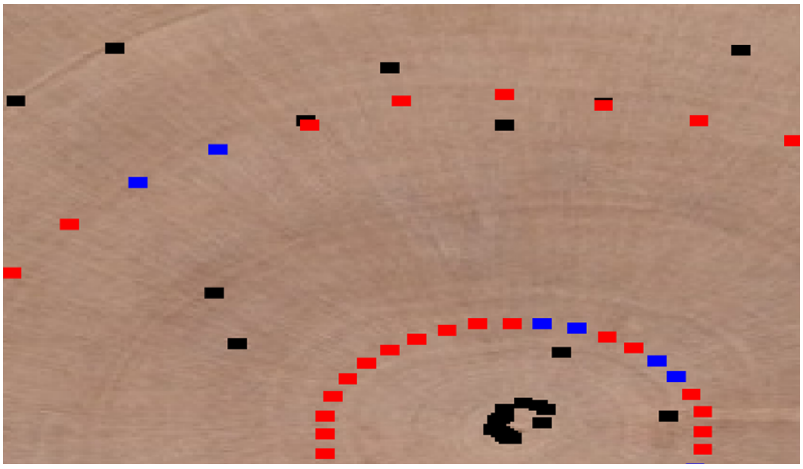

Fig. 6. Magnified view of the cross-sectional region of the tree from the species Retrophyllum rospigliosii demarcated by color intensity gradient. The irregular coloring observed in the cross-sectional wood section influences the selection of candidate points that could constitute the growth ring.
Source: Authors.

Semi-automatic method: Figure 7 illustrates a portion of the results obtained using the semi-automatic demarcation method applied to the cross-sectional image of a Retrophyllum rospigliosii tree. The local Laplacian and Frangi filters are used to evaluate the orientation of edge pixels at specific radial distances from the center and to identify potential ring edge candidates. A subsequent Sobel filter is then applied to refine these candidates. Candidate pixels are displayed in red, while their eight nearest neighbors—forming a 3×3 matrix—are shown in green. Each pixel in this matrix is a potential contributor to the complete contour of the growth ring.

The user may accept the red candidate, select a more suitable neighbor, or add new candidates if the automated filtering fails to detect the correct ring edge at a given angle. Once accepted, ring edge candidates are colored magenta. This process is then repeated for the next angle.

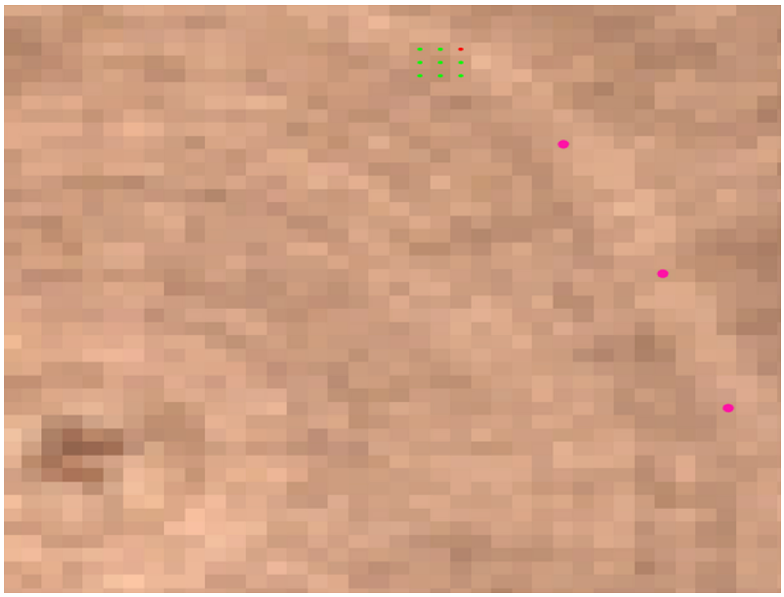

Fig. 7. Magnified view of the cross-sectional region of the tree from the species Retrophyllum rospigliosii with semi-automatic demarcation. The magenta points represent the user's selection. The selection of points is contingent upon the user's expertise in identifying growth rings in tropical conifers.

Source: Authors.

Width of rings: Table 1 presents the growth ring widths obtained using the different methods evaluated in this study, applied to the cross-sectional image of a Retrophyllum rospigliosii tree. The techniques assessed include the gradient of color difference and the semi-automatic demarcation method. To evaluate their accuracy, the percentage error was calculated by taking the absolute difference between the

e-ISSN 2357-6014 / Vol. 21, no. 2 / may-august 2025 / Bogotá D.C., Colombia
Universidad Cooperativa de Colombia

value obtained by the tested method and the manually measured reference value, dividing it by the reference value, and multiplying by 100.

For both methods shown in Table 1, the selected rays correspond to those used in the manual tracing to ensure a valid comparison. The width measurements are expressed in millimeters, based on the known resolution of the scanner used to digitize the samples.

TABLE 1. Width of growth rings in millimeters and percent error for each method described. Values marked with dashes indicate that the method used could not detect growth rings for the ray traced in that ring.

Rings	Manual (Reference) (mm)	Color Difference Gradient (mm)	% Color Difference Gradient Error	Semiautomatic Demarcation (mm)	% Semiautomatic Demarcation Error
1	5.46	5.00	8.42	5.41	0.92
2	3.44	12.62	266.86	3.33	3.20
3	4.32	12.62	192.13	4.73	9.49
4	2.50	12.62	404.80	2.58	3.20
5	2.78	-	-	3.74	34.53
6	2.30	-	-	2.05	10.87
7	4.72	-	-	4.25	9.96
8	2.24	-	-	1.21	45.98
9	4.42	-	-	3.18	28.05
10	5.90	-	-	5.92	0.34
11	0.62	-	-	1.48	138.71
12	7.62	-	-	7.41	2.76
13	4.28	-	-	5.34	24.77
14	2.86	-	-	2.20	23.08
15	5.16	-	-	4.15	19.57
16	1.32	-	-	1.66	25.76
17	2.12	-	-	0.67	68.40
18	0.60	-	-	0.75	25.00
19	0.58	-	-	0.21	63.79
20	0.70	-	-	0.35	50.00

The root mean squared error (RMSE) was calculated to compare the average error in millimeters for the ring widths identified using the color difference gradient method and the semi-automatic method. The results, rounded to two decimal places, were: RMSE = 8.00 mm for the gradient method and RMSE = 0.70 mm for the semi-automatic method. In addition, the mean absolute percentage error (MAPE) was

computed, yielding approximate values of MAPE = 218.05% for the gradient method and MAPE = 29.42% for the semi-automatic method.

Figure 8 compares the percentage error and ring widths obtained through the manual and semi-automatic methods (as detailed in Table 1), providing a basis for evaluating the effectiveness of the semi-automatic approach. The semi-automatic method demonstrates a considerably lower error rate, with an average percentage error close to 30% across different rings, highlighting its improved accuracy and reliability compared to the fully automatic approach.

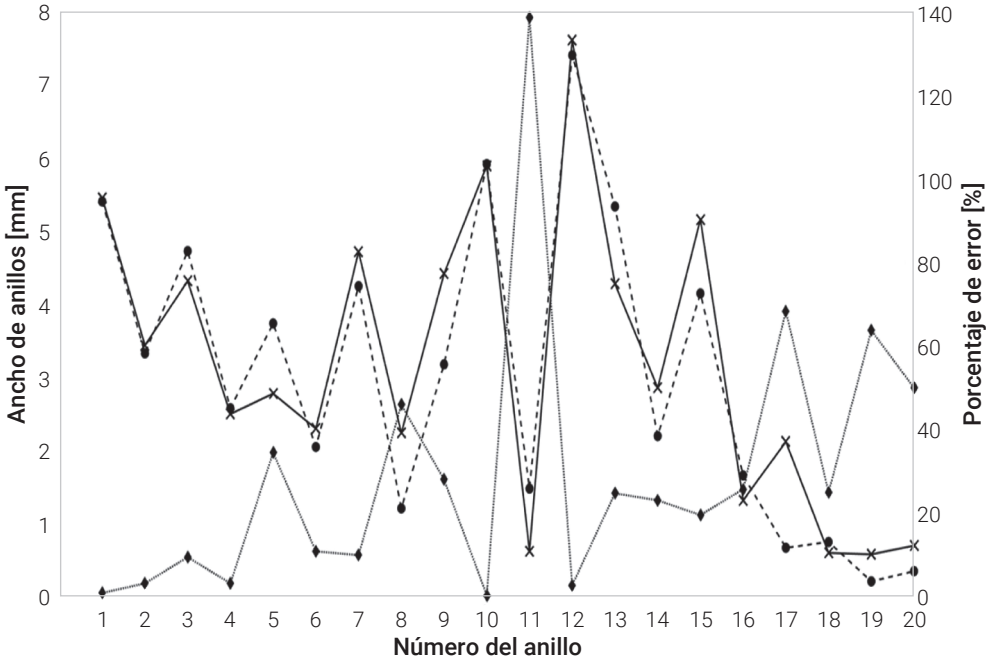

Fig. 8. Percent error for each ring along a ray from the pith to the bark of a Retrophyllum rospigliosii trunk section, comparing the described methods. The semi-automatic method successfully detects all 20 rings, consistent with the known age of the 20-year-old trunk. The dotted line shows the percentage error for each ring (right axis), the solid line represents the manually measured ring widths in millimeters (left axis), and the dashed line displays the ring widths obtained using the proposed semi-automatic method (left axis).

Source: Authors.

4. DISCUSSION AND CONCLUSIONS

Research has demonstrated that manual demarcation of growth rings is possible for tropical tree species like Retrophyllum rospigliosii, despite their poorly defined growth rings. This highlights the dendroecological potential of this species [25].

e-ISSN 2357-6014 / Vol. 21, no. 2 / may-august 2025 / Bogotá D.C., Colombia
Universidad Cooperativa de Colombia

However, the standard process for automated ring marking and measurement typically involves the following steps: first, capturing a high-resolution digital color image of the tree cross-section under uniform lighting to minimize shadow artifacts. For this reason, scanning is a common procedure in this field [26], [27]. The image is then transformed to grayscale, possibly after conversion to other color spaces that emphasize hue differences, such as HSV or CIELab. Next, edge-preserving smoothing is applied using algorithms like the Gaussian filter. To highlight pixels forming growth rings, the following steps are used: iv) applying filters such as the Sobel operator or Canny edge detector, v) separating ring pixels from background or adjacent rings using thresholding or image segmentation techniques—ranging from basic histogram thresholding to classification using neural networks or machine learning algorithms, and vi) calculating distances between ring edge pixels [16].

Applying automatic ring demarcation to this species using conventional methods presents a significant challenge in computer vision. This is due to the minimal differentiation between ring edge pixels and background pixels. Growth rings are very narrow, and in some radial segments of the image, edge pixels may be nearly absent. This difficulty is reflected in the high average percentage error (218.05%) obtained using the proposed color intensity gradient algorithm.

One of the main challenges faced by automatic algorithms is their inability to distinguish growth rings along all rays traced from the core to the outer bark, due to the low hue contrast between ring and background pixels. Even with erosion and dilation techniques, edge detection filters such as Sobel or Canny often produce unsatisfactory results. In contrast, an expert user can compare rays from other regions of the trunk. This study proposes a semi-automatic tool to assist such users in identifying growth rings. The tool presents a set of candidate pixels for ring edges, which the user can confirm or reject. Additionally, the user can mark missing pixels if they believe the automatic filter has failed to detect a ring edge at a specific angle.

This procedure yielded results more consistent with the manual method, with an average percentage error of 29.42% and an average absolute error of 0.17 millimeters. The curves in Figure 8 demonstrate this consistency across all rings.

Furthermore, while the automatic method correctly identified only 4 of the 20 growth rings corresponding to the tree's age, the semi-automatic method identified all 20, although this depends to some extent on the user's experience.

These difficulties have also been noted in other studies, such as [28], where X-ray tomography was proposed as a solution.

Scanner-based image analysis tools have the potential for wider application compared to those based on microscopy or X-ray tomography. However, the main

limitation of the semi-automatic approach lies in its reliance on experienced users, representing only a modest improvement over manual measurement. Improving the proposed algorithm to reduce ring width measurement errors could involve integrating supervised pattern recognition techniques. These techniques could be trained on user inputs—accepting or rejecting candidate pixels—in the pursuit of a more efficient automatic solution.

Developing effective methods for ring demarcation in tropical species like Retrophyllum rospigliosii is essential for realizing their dendrochronological potential to investigate climatic phenomena in regions lacking consolidated climate records. This could contribute to climate prediction and forest conservation in areas affected by irregular dry and rainy seasons.

REFERENCES

[1] C. F. Fortes, C. N. d-Cunha, S. A. Rosa, E. Paixao, W. J. Junk, and J. Schogart, "Dendrochronological records of a pioneer tree species containing ENSO signal in the Pantanal, Brazil," *Brazilian Journal of Botany*, vol. 41, pp. 167–174, 2018, doi: https://doi.org/10.1007/s40415-017-0434-8.

[2] F. Wu, Y. Huang, B. Benes, C. C. Warner, and R. Gazo, "Automated tree ring detection of common Indiana hardwood species through deep learning: Introducing a new dataset of annotated images," *Information Processing in Agriculture*, pp. 247–254, Nov. 2023, doi: https://doi.org/10.1016/j.inpa.2023.10.002.

[3] J. A. Giraldo Jiménez, "Dendrocronología en el trópico: aplicaciones actuales y potenciales dendrocronology in the tropics: current and potential applications," *Colombia Forestal*, vol. 14, no. 1, pp. 97–111, 2011.

[4] A. Quesada-Román, J. A. Ballesteros-Cánovas, S. St. George, and M. Stoffel, "Tropical and subtropical dendrochronology: Approaches, applications, and prospects," *Ecological Indicators*, vol. 144, pp. 65–80, Nov. 2022, doi: https://doi.org/10.1016/j.ecolind.2022.109506.

[5] M. H. Calp and U. Kose, "Estimation of burned area in forest fires using artificial neural networks," *Ingeniería Solidaria*, vol. 16, no. 3, pp. 1–22, Sep. 2020, doi: https://doi.org/10.16925/2357-6014.2020.03.08.

[6] V. L. Caetano-Andrade et al., "Tropical trees as time capsules of anthropogenic activity," *Trends in Plant Science*, vol. 25, no. 4, pp. 369–380, Apr. 2020, doi: https://doi.org/10.1016/j.tplants.2019.12.010.

[7] M. Worbes, "Mensuration | Tree-ring analysis," in *Encyclopedia of Forest Sciences*. Amsterdam, Netherlands: Elsevier, 2004, pp. 586–599, doi: https://doi.org/10.1016/B0-12-145160-7/00059-4.

[8] D. Granato-Souza et al., "Tree rings and rainfall in the equatorial Amazon," *Climate Dynamics*, vol. 52, no. 3–4, pp. 1857–1869, Feb. 2019, doi: https://doi.org/10.1007/s00382-018-4227-y.

[9] A. Fabijańska and M. Danek, "DeepDendro – A tree rings detector based on a convolutional neural network," *Computers and Electronics in Agriculture*, vol. 150, pp. 353–363, Jul. 2018, doi: https://doi.org/10.1016/j.compag.2018.05.005.

[10] A. Venegas-González et al., "What tree rings can tell us about the competition between trees and lianas? A case study based on growth, anatomy, density, and carbon accumulation," *Dendrochronologia (Verona)*, vol. 42, pp. 1–11, Mar. 2017, doi: https://doi.org/10.1016/j.dendro.2016.11.001.

[11] R. J. DeRose, J. N. Long, and R. D. Ramsey, "Combining dendrochronological data and the disturbance index to assess Engelmann spruce mortality caused by a spruce beetle outbreak in southern Utah, USA," *Remote Sensing of Environment*, vol. 115, no. 9, pp. 2342–2349, Sep. 2011, doi: https://doi.org/10.1016/j.rse.2011.04.034.

[12] A. Quesada-Román, J. A. Ballesteros-Cánovas, S. St. George, and M. Stoffel, "Tropical and subtropical dendrochronology: Approaches, applications, and prospects," *Ecological Indicators*, vol. 144, pp. 100–114, Nov. 2022, doi: https://doi.org/10.1016/j.ecolind.2022.109506.

[13] J. Björklund, K. Seftigen, P. Fonti, D. Nievergelt, and G. von Arx, "Dendroclimatic potential of dendroanatomy in temperature-sensitive *Pinus sylvestris*," *Dendrochronologia (Verona)*, vol. 60, p. 125673, 2020, doi: https://doi.org/10.1016/j.dendro.2020.125673.

[14] P. Hietz, "A simple program to measure and analyse tree rings using Excel, R and SigmaScan," *Dendrochronologia (Verona)*, vol. 29, no. 4, pp. 245–250, 2011, doi: https://doi.org/10.1016/j.dendro.2010.11.002.

[15] J. Van den Bulcke et al., "Advanced X-ray CT scanning can boost tree-ring research for earth-system sciences," *Annals of Botany*, vol. 124, no. 5, pp. 837–847, 2019, doi: https://doi.org/10.1093/aob/mcz126.

[16] S. Subah, S. Derminder, and C. Sanjeev, "An interactive computer vision system for tree ring analysis," *BMC Genomics*, vol. 112, no. 6, pp. 16–21, 2017, doi: https://doi.org/10.1186/s12864-015-1373-z.

[17] P. M. Sundari, S. B. R. Kumar, and A. J. Sahayaraj, "An approach for analyzing the factors recorded in the tree rings using image processing techniques," in *Proc. 2nd World Congr. on Computing and Communication Technologies (WCCCT)*, 2017, pp. 236–239, doi: https://doi.org/10.1109/WCCCT.2016.65.

[18] S. Arenas-Castro, J. Fernández-Haeger, and D. Jordano-Barbudo, "A method for tree-ring analysis using Diva-Gis freeware on scanned core images," *Tree-Ring Research*, vol. 71, no. 2, pp. 118–129, 2015, doi: https://doi.org/10.3959/1536-1098-71.2.118.

[19] W. Lara, F. Bravo, and C. A. Sierra, "MeasuRing: An R package to measure tree-ring widths from scanned images," *Dendrochronologia (Verona)*, vol. 34, pp. 43–50, 2015, doi: https://doi.org/10.1016/j.dendro.2015.04.002.

[20] M. A. Stokes and T. L. Smiley, *An Introduction to Tree-Ring Dating*. Chicago, IL: University of Chicago Press, 1968, pp. 1–10.

[21] Science Education Resource Center, "TREX Tree-Rings Expeditions, Part 3: Measuring and graphing tree-ring width at Chaco Canyon, NM," Accessed: Nov. 28, 2023. [Online]. Available: https://serc.carleton.edu/trex/students/labs/lab3_3.html

[22] B. Zhu, J. Liu, R. Pan, S. Wang, and W. Gao, "Fabric seam detection analysis using wavelet transform and CIELAB color space: A comparison," *Optik (Stuttgart)*, vol. 126, no. 24, pp. 5650–5655, Dec. 2015, doi: https://doi.org/10.1016/j.ijleo.2015.08.163.

[23] A. F. Frangi, W. J. Niessen, P. J. Nederkoorn, J. Bakker, W. P. T. M. Mali, and M. A. Viergever, "Quantitative analysis of vascular morphology from 3D MR angiograms: In vitro and in vivo results," *Magnetic Resonance in Medicine*, vol. 45, no. 2, pp. 311–322, 2001, doi: https://doi.org/10.1002/1522-2594(200102)45:2<311::AID-MRM1040>3.0.CO;2-7.

[24] D.-J. Kroon, "Hessian based Frangi vesselness filter," *MATLAB Central File Exchange*, 2010.

[25] M. Escobar, A. Marín, J. A. Giraldo, and J. Ramírez, "Potencial dendrocronológico de tres especies de Podocarpáceas de la Cordillera de los Andes," *Revista de Biología Tropical*, vol. 71, pp. 127–140, 2023, doi: https://doi.org/10.15517/rev.biol.trop.v71i1.54971.

[26] D. Kim, C. U. Ko, and D. Kim, "Method for detecting tree ring boundary in conifers and broadleaf trees using Mask R-CNN and linear interpolation," *Dendrochronologia (Verona)*, vol. 79, pp. 17–30, Jun. 2023, doi: https://doi.org/10.1016/j.dendro.2023.126088.

[27] R. Shikangalah et al., "Growth rings and stem diameter of *Dichrostachys cinerea* and *Senegalia mellifera* along a rainfall gradient in Namibia," *Trees, Forests and People*, vol. 3, pp. 101–114, Mar. 2021, doi: https://doi.org/10.1016/j.tfp.2020.100046.

[28] J. Martinez-Garcia, I. Stelzner, J. Stelzner, D. Gwerder, and P. Schuetz, "Automated 3D tree-ring detection and measurement from X-ray computed tomography," *Dendrochronologia (Verona)*, vol. 69, pp. 360–373, Oct. 2021, doi: https://doi.org/10.1016/j.dendro.2021.125877.